Subband densities in quantum wells under in-plane magnetic fields

G. Salis, B. Ruhstaller, and K. Ensslin
Solid State Physics Laboratory, ETH Zürich, 8093 Zürich, Switzerland

K. Campman, K. Maranowski, and A. C. Gossard
Materials Department, University of California, Santa Barbara, California 93106
(Received 2 February 1998; revised manuscript received 6 April 1998)

The dependence of the subband densities in a potential well with tunable symmetry on a weak in-plane magnetic field is investigated experimentally by analyzing Shubnikov–de Haas oscillations. We measure a strong carrier redistribution between the subbands, which is explained by individual magnetic-field–dependent density of states in different subbands rather than by the diamagnetic energy shift. The measured carrier redistribution is quantitatively explained considering the in-plane field in second-order perturbation theory. [S0163-1829(98)07927-2]

I. INTRODUCTION

An electron system confined in one spatial dimension with an additional magnetic field is a textbook example that allows one to study the behavior of quantum-mechanical energy levels and wave functions in detail. If the magnetic field is oriented perpendicularly to the plane of the electron system, the Hamiltonian can be separated with respect to the in-plane and perpendicular motion. Therefore the Landau quantum numbers and subband quantum numbers are independent of each other and level degeneracies occur at certain magnetic fields.[1] In the case of a parabolic confining potential, the Hamiltonian can be solved analytically for any orientation of the magnetic field.[2,3] For arbitrary confining potentials one relies on perturbative approaches. A lot of theoretical[4–13] as well as experimental work has been done in this field.[14–17] In this paper we focus on the importance of second-order perturbation theory for a small—but arbitrarily oriented—magnetic field. In particular we find a strong redistribution of the subband electron densities due to an in-plane magnetic field, which we quantitatively explain by a subband-dependent density of states.

The in-plane field has two effects: The energy levels are diamagnetically shifted, and the dispersion relation of the in-plane electron motion is modified, which can be described by a magnetic-field–dependent effective mass.[5,12,16] Thus the two-dimensional density of states (DOS) depends on the in-plane magnetic field.

Experimentally, the electron densities n_i of the subbands i in the presence of an in-plane magnetic field $B_\parallel$ can be determined by analyzing Shubnikov–de Haas (SdH) oscillations in a transport measurement. In the case of one occupied subband, the diamagnetic shift of the subband energy has no influence on the measured subband density. However, the modified effective mass can be determined by measuring the temperature dependence of the SdH oscillations[18,19] or by optical experiments.[16] Only if more than one subband is populated, the diamagnetic energy shift may lead to a redistribution of subband densities. The parallel-field dependence of n_i has been measured for heterojunctions[15] and for parabolic quantum wells.[19] In Refs. 19, measurements of a parabolic quantum well (PQW) were compared with the analytical solution of the parabolic confining potential, although the effective potential is closer to a rectangular well. In order to compare the measured $n_i(B_\parallel)$ with the diamagnetic energy shift, a perturbative expression for the diamagnetic shift was considered in Ref. 14 and 15. However, the varying DOS was not taken into account. As was pointed out in Ref. 9, the varying DOS can have a significant effect on the depopulation of the upper subband.

In this paper, we present measurements confirming that the influence of the $B_\parallel$-dependent DOS on the measured subband densities may be dominant over the diamagnetic shift. We have measured $B_\parallel$ dependencies of subband densities in a wide PQW with tunable electron sheet density and potential symmetry. The effect of these parameters on n_i is studied for small $B_\parallel$. The data are compared with a perturbative calculation of the energies to second order, using self-consistently calculated wave functions at $B=0$ as a basis. The first-order term determines the diamagnetic shift, whereas distortions of the Fermi sphere are due to the second-order term. As we will show, the latter effect on n_i is of the same order of magnitude as the diamagnetic shift. It may even dominate the $B_\parallel$ dependence of n_i in the case when the DOS in the individual subbands differ. By applying a front-gate bias, we experimentally control the difference between the subband-dependent DOS and study its influence on the measured subband densities.

II. EXPERIMENT

The investigated samples contain a 760-Å wide and 79-meV-deep $Al_xGa_{1-x}As/GaAs$ parabolic quantum well grown by molecular beam epitaxy. The well is remotely doped with Si on both sides. Back- and front-gate electrodes allow a controlled variation of both electron density and potential symmetry. In order to increase the asymmetry induced by the front-gate bias, a 3-ML-thick $Al_{0.15}Ga_{0.85}As$ spike is situated in the center of the well. The detailed sample layout is described in Ref. 20. A standard Hall-bar geometry was used for transport measurements.

The sample was mounted on a revolving stage. Measure-

 © 1998 The American Physical Society

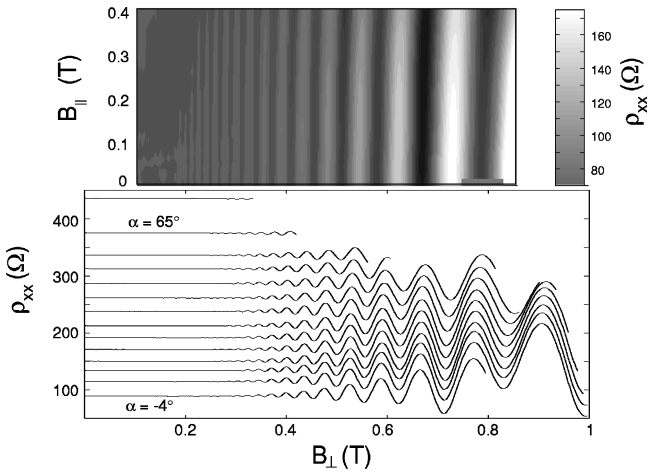

FIG. 1. Measured magnetoresistances ρ_{xx} as a function of the perpendicular field $B_\perp$ for different tilt angles α between $-4°$ and 65°. The ρ_{xx} values are offset for clarity. The upper part of the figure shows a contour plot of the same data as a function of $B_\parallel$ and $B_\perp$. Darker regions correspond to higher ρ_{xx} (the grey scale is indicated on the right side).

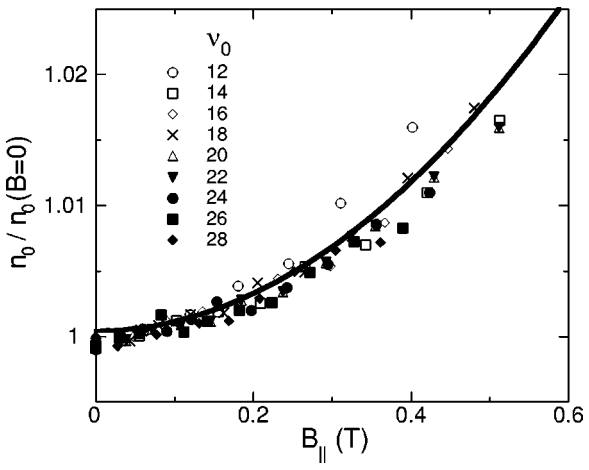

FIG. 2. Density of the lowest subband n_0 normalized to the density $n_0(B_\parallel=0)$ as a function of the in-plane field, as obtained from measurements presented in Fig. 1. For the determination of n_0, filling factors of the E_0 subband between 12 and 28 and tilt angles between $-4°$ and 65° have been evaluated.

ments were performed at 1.7 K. The tilt angle α between the sample normal and the direction of the magnetic field was determined by scaling both the Hall resistance ρ_{xy} and the Shubnikov–de Haas (SdH) minima in the magnetoresistance ρ_{xx} to $\cos\alpha$ (with the sample being in the single-subband regime). We estimate the accuracy of the obtained angle α to be better than 0.2°.

In the case of two occupied subbands E_0 and E_1 (densities n_0 and n_1), the SdH minima do not scale with $\cos\alpha$ anymore. In a weak perpendicular field $B_\perp$, ρ_{xx} is periodic in $1/B_\perp$ with a frequency proportional to n_0. The oscillation due to the E_1 subband is weak and not observed for low densities n_1 (Fig. 1). If the sample is tilted by an angle α, the degeneracy of each Landau level is still determined by $B_\perp$. Analyzing the $B_\perp$ positions of even filling factors allows one to determine n_0 in tilted fields.

Figure 1 shows measured traces of ρ_{xx} plotted as a function of the perpendicular magnetic field $B_\perp = B\cos\alpha$ with the tilt angle α as a parameter. As there is no spin splitting observed at low magnetic fields, each minimum in $\rho_{xx}(B_\parallel)$ corresponds to an even E_0 subband filling factor ν_0, which is deduced from the ρ_{xx} trace at $\alpha=0$. The subband density $n_0 = e\nu_0 B_\perp/h$ is determined by the $B_\perp$ position of such a minimum. In Fig. 2, we present n_0 as a function of the in-plane field $B_\parallel$ by using $B_\parallel = B_\perp \tan\alpha$. Several filling factors ν_0 between 12 and 28 and tilt angles α between $-4°$ and 65° have been evaluated. In the case of two occupied subbands, n_0 generally increases with $B_\parallel$, corresponding to a depletion of the upper subband.[15,21] We limit the discussion to small magnetic fields $B_\parallel, B_\perp < 1$ T. To first order, the increase of n_0 is quadratic in $B_\parallel$. We therefore introduce the coefficient $\gamma = dn_0/dB_\parallel^2$, which we determine from a parabolic fit to the measured data.

Of interest here is the variation of γ with the total density and the symmetry of the well. For this purpose, measurements as presented in Fig. 2 were performed for different front-gate biases $V_{\rm fg}$. The total sheet density n_S increases with $V_{\rm fg}$ and the electron distribution moves closer to the sample surface. Figure 3 presents the measured γ, plotted as a function of n_S. Note that the potential symmetry also changes with n_S, due to the inserted potential spike and the boundaries of the well. Up to densities around $n_S = 3.0\times10^{15}$ m^{-2}, γ increases and reaches a maximum value of 1.7×10^{14} m^{-2} T^{-1}.

In the following section, we compare the data with a perturbative calculation of the diamagnetic shift and the DOS, and with the analytical solution for a parabolic confining

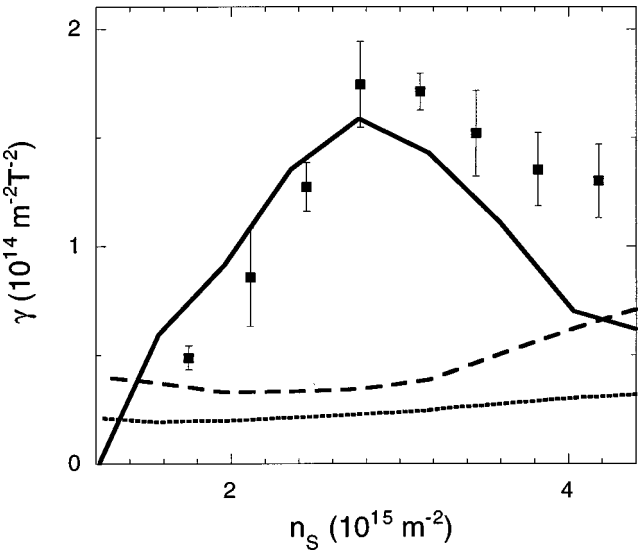

FIG. 3. Measured change of density per magnetic field $\gamma = dn_0/dB_\parallel^2$ as a function of the sheet density n_S (symbols). Note that n_S is varied by applying a front-gate bias, and thus also the symmetry is changed with increasing n_S. A maximum of γ is observed near $n_S = 3.0\times10^{15}$ m^{-2}. The error bars indicate deviations in γ originating from evaluation with different filling factors. The dotted line corresponds to the first-order perturbation theory [Eq. 3], which is up to seven times smaller than the measured values. The full line indicates the full second-order calculations, the dashed line the first term $\Delta n[\,\delta/2+(\beta_0+\beta_1)/4]$, which neglects subband-dependent DOS.

potential. It will be shown that the $B_\parallel$ dependence of the DOS results in up to five times higher values for γ. Only if this $B_\parallel$ dependence—obtained by the second-order term of the perturbation calculation—is included, the calculation can quantitatively account for the measured γ.

III. COMPARISON WITH THEORY

A. First-order perturbation theory

In the following we calculate the energy spectrum of a two-dimensional electron system subjected to an in-plane field $B_\parallel$. The perpendicular field has not to be included in the calculation, as we use small fields, where the Landau ladder is smoothed out to an approximately constant DOS. A perturbative calculation of the effective cyclotron mass m^* in tilted fields is presented in Ref. 16, where the $B_\parallel$ dependence of m^* originates from a shift in Landau-level separation due to the coupling Hamiltonian. The effective mass obtained from the Landau-level spacing is equivalent to that considering the dispersion modification due to an in-plane field.

With the vector potential $\mathbf{A}=(0,-B_\parallel z,0)$, the momentum operator p_z in the z direction, the elementary charge e, and electron effective mass m^*, the Hamiltonian of noninteracting electrons mobile in the x-y plane and confined in the z direction by a potential $V(z)$ is found to be

$$H=\underbrace{\frac{p_z^2}{2m^*}+V(z)}_{H_0}+\frac{\hbar^2k_x^2}{2m^*}+\frac{\hbar^2k_y^2}{2m^*}+\underbrace{\frac{e^2B_\parallel^2}{2m^*}z^2+\frac{eB_\parallel\hbar k_y}{m^*}z}_{H'}. \tag{1}$$

The wave function is separated into plane waves along the x and y directions (wave numbers k_x and k_y) and the solution $\phi_i(z,k_y)$ to H_0+H' with energy $E_i(k_y)$. The total energy is given by $E_i(k_x,k_y)=E_i(k_y)+\hbar^2(k_x^2+k_y^2)/2m^*$. Nondegenerate perturbation theory is applied to the eigenstates of H_0 with energies E_i^0 and wave functions ϕ_i^0, treating H' as a small perturbation (small in-plane fields $B_\parallel$). The first-order correction to the energy results in

$$E_i(k_x,k_y)\approx E_i^0+\frac{\hbar^2k_x^2}{2m^*}+\frac{\hbar^2(k_y-k_0)^2}{2m^*}+\frac{e^2B_\parallel^2}{2m^*}(\langle z^2\rangle_{ii}-\langle z\rangle_{ii}^2), \tag{2}$$

where $\langle\cdots\rangle_{ij}$ denotes the matrix elements corresponding to the wave functions ϕ_i^0 and ϕ_j^0, respectively, and $k_0=eB_\parallel\langle z\rangle_{ii}/\hbar$. The diamagnetic shift in energy[4] is quadratic in $B_\parallel$ and proportional to $\langle z^2\rangle-\langle z\rangle^2$. The magnitude of the shift increases with subband number i due to the increasing spatial extent of higher subband wave functions. Additionally, the Fermi surface is displaced in the x direction by k_0. This displacement has no influence on the DOS and the effective mass m^*. Thus the magnetic-field dependence of the subband density $n_0=m^*/\pi\hbar^2(E_F-E_0)$ is given by the $B_\parallel$ dependence of E_0 and E_F. The Fermi energy E_F depends on $B_\parallel$ because of the rearrangement of subband densities. In the following, we assume that two subbands E_0 and E_1 are occupied ($E_F>E_0,E_1$). With $\Delta n=n_0-n_1|_{B_\parallel=0}$, we obtain for $\gamma=dn_0/dB_\parallel^2$

$$\gamma=\Delta n\frac{\delta}{2}, \tag{3}$$

with

$$\delta=\frac{e^2}{2m^*}\frac{\langle z^2-\langle z\rangle^2\rangle_{11}-\langle z^2-\langle z\rangle^2\rangle_{00}}{E_1^0-E_0^0}. \tag{4}$$

By solving the Poisson and Schrödinger equations for our PQW self-consistently, we find the wave functions ϕ_i^0 and energies E_i^0 for different gate biases. The consistency of these values can be checked by comparing the obtained E_i^0 with the measured subband densities n_i at zero in-plane field, divided by the DOS.[1] In a previous paper we have demonstrated good agreement between calculated data and experimentally obtained energy levels and wave functions.[20] If the calculated ϕ_i^0 and E_i^0 are inserted into Eq. (3), one obtains values for γ that are up to 7 times smaller than the measured ones (Fig. 3).

B. Second-order term and subband-dependent DOS

We have to take into account second-order perturbation theory. Neglecting powers of $B_\parallel$ larger than two leads to the following corrections to $E_i(k_x,k_y)$:

$$E_i''(k_y)=-\frac{\hbar^2k_y^2}{m^*}\beta_iB_\parallel^2 \tag{5}$$

with

$$\beta_0=\frac{e^2}{m^*}\frac{\langle z\rangle_{10}^2}{E_1^0-E_0^0},$$

$$\beta_1=\frac{e^2}{m^*}\frac{\langle z\rangle_{21}^2}{E_2^0-E_1^0}-\beta_0. \tag{6}$$

This second-order term leads to a modified dispersion relation in the y direction $\hbar^2k_y^2/2m_y^*$ with $m_y^*=m^*/(1-2\beta_iB_\parallel^2)$, whereas the x direction remains unaffected. This signifies that the Fermi sphere is distorted to an ellipsoid, which can be accounted for by a modified, subband-dependent effective mass[5,9]

$$m_i^*=\sqrt{m_x^*m_y^*}\approx m^*(1+\beta_iB_\parallel^2). \tag{7}$$

Therefore the DOS depends on $B_\parallel$ and on the subband index i:

$$D_i=D(1+\beta_iB_\parallel^2). \tag{8}$$

In the equations above we assumed that $\beta_iB_\parallel^2\ll1$, which is a prerequisite for the applicability of perturbation theory. The parameter β is proportional to the ratio of Landau energy $\hbar eB_\parallel/m^*$ and subband energy difference, as well as on $\langle z\rangle_{10}^2/l_{B_\parallel}^2$ with the squared magnetic length $l_{B_\parallel}^2=\hbar/eB_\parallel$. Thus both the Landau energy compared to the subband difference,

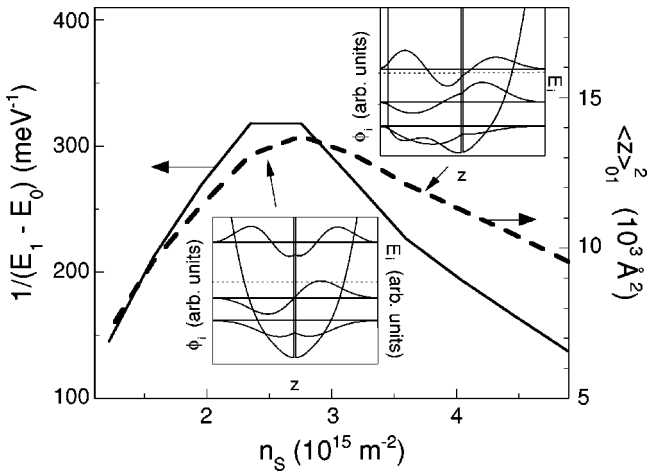

FIG. 4. Calculated values for $(E_1^0 - E_0^0)^{-1}$ and $\langle z \rangle_{10}^2$ for different sheet densities n_S. The dominating contribution to γ originating from the second-order term is proportional to $\langle z \rangle_{10}^2/(E_1^0 - E_0^0)$. The insets show the self-consistent potential, the wave functions ϕ_i^0 and the energy levels E_i^0 for subbands $i = 0,1,2$ and for two different densities n_S.

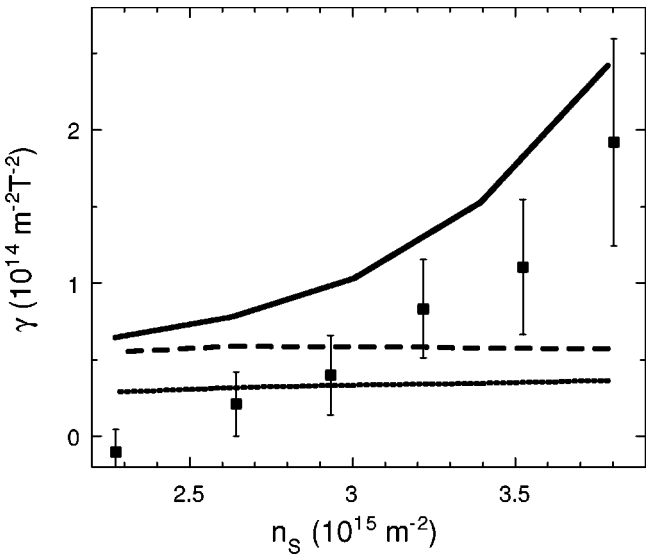

FIG. 5. Measured values of γ (symbols) for different n_S compared to results from second-order perturbation theory (line) for a sample with a weak potential spike (Al content $x = 0.05$, width 8.5 Å) centered in the potential well. The error bars correspond to evaluations at different filling factors. The dotted line describes the diamagnetic shift only, the dashed line includes the $\beta_0 + \beta_1$ term.

and the off-diagonal z-matrix element compared with the magnetic length have to be small for the applicability of perturbation theory.

In the approximation used here, the subband-dependent correction to the DOS varies quadratically with the in-plane field. In the description of the subband density, we therefore have to be careful in converting the energy levels to subband densities. The subband densities are written as $n_i = D_i(E_F - E_i)$. With $n_S = n_0 + n_1$ we obtain for γ:

$$\gamma = \Delta n \left(\frac{\delta}{2} + \frac{\beta_0 + \beta_1}{4} \right) + n_S \frac{\beta_0 - \beta_1}{4}. \tag{9}$$

In the first term we recognize the first-order result of Eq. (3), with δ replaced by $\delta + (\beta_0 + \beta_1)/2$. As we will show in the next section, this corresponds to a doubled value in the case of a parabolic confining potential. Because of the increase in the DOS with $B_\parallel^2$, more carriers accommodate in the lower subband, which gives rise to an increase in n_0 of the same order as from the diamagnetic shift itself.

The second term being proportional to the sheet density n_S and the difference of the DOS parts β_0 and β_1 cancels out in an exact parabolic potential. For arbitrary potentials though, the $B_\parallel$ dependence of the DOS can be quite different for the two subbands, leading to an additional redistribution of the carrier densities between the two subbands. The influence of this term on $n_0(B_\parallel)$ can even dominate.

If we insert the calculated ϕ_i^0 and E_i^0 into Eq. (6) and (9), we in fact observe strongly different β_i and the second term of Eq. (9) dominates the resulting γ (Fig. 3). In contrast to the first-order result, this calculation is in good agreement with the experimental values, and perfectly reproduces the maximum around $n_S = 3.0 \times 10^{15}$ m^{-2}.

C. Exact solution for a parabolic potential

In the exact solution for a parabolic quantum well with potential $V(z) = m^* \Omega^2 z^2/2$, the subband energy levels for an in-plane field $B_\parallel$ are given by[2,3] $E_n = \hbar(\omega_c^2 + \Omega^2)^{1/2}$ $(n + 1/2)$, with the cyclotron frequency $\omega_c = eB_\parallel/m^*$. The DOS is independent of the subband number and is found to be

$$D(B_\parallel) = D\left(1 + \frac{\omega_c^2}{\Omega^2} \right)^{1/2}. \tag{10}$$

Thus one obtains for γ

$$\gamma = D\hbar\Omega \frac{e^2}{2m^{*2}\Omega^2}. \tag{11}$$

Considering that $\langle z \rangle_{10}^2 = \hbar/2m^*\Omega$, $\langle z \rangle_{21}^2 = \hbar/m^*\Omega$ and $\langle z^2 \rangle_{11} - \langle z^2 \rangle_{00} = \hbar/m^*\Omega$, we recover exactly the result of Eqs. (6) and (8). It is worth noting that in the case of a parabolic potential the perturbation theory up to order $B_\parallel^2$ gives the exact result. Considering Eq. (9), we find that $(\beta_0 + \beta_1)/2 = \delta$, and $\beta_0 - \beta_1 = 0$. Thus the second-order result is exactly twice the first-order result of Eq. (3), and the term proportional to n_S in Eq. (9) vanishes.

IV. DISCUSSION AND CONCLUSIONS

The data presented in Fig. 3 provides evidence that the $B_\parallel$-driven carrier redistribution among the two subbands is dominated by the $B_\parallel$-dependent DOS. We observe a maximum in $\gamma(n_S)$ that is due to a subband specific DOS, described by the term in Eq. (9) containing $\beta_0 - \beta_1$. Using Eq. (6) one finds that

$$\beta_0 + \beta_1 \propto \frac{\langle z \rangle_{21}^2}{E_2^0 - E_1^0} \tag{12}$$

and

TABLE I. Calculated contributions to the subband carrier redistribution γ for a heterostructure, a parabolic potential, a PQW without and with spike as measured, and a double quantum well (DQW). γ is split into the diamagnetic shift part γ_{dia} (containing δ) and the DOS part γ_{DOS} (containing β_0 and β_1). In the DQW and PQW the wave functions are centered in the well.

Sample	2δ (T^{-2})	$\beta_0+\beta_1$ (T^{-2})	$\beta_0-\beta_1$ (T^{-2})	n_S (10^{15} m^{-2})	n_0-n_1 (10^{15} m^{-2})	γ_{dia} (10^{14} m^{-2} T^{-2})	γ_{DOS} (10^{14} m^{-2} T^{-2})
Heterostructure [a]	0.013	0.032	−0.027	4.9	4.6	0.15	0.04
parabolic potential	0.024	0.024	0	3.2-6.4	3.2	0.19	0.19
PQW	0.104	0.080	0.058	2.8	1.3	0.34	0.67
PQW+spike	0.128	0.045	0.181	2.8	0.9	0.29	1.37
DQW [b]	0.011	0.001	0.311	5.2	0.4	0.01	4.04

[a]Spacer layer 100 Å, residual acceptor concentration 2.7×10^{20} m^{-3}, donor layer 6.5×10^{15} m^{-2}.
[b]Well width 140 Å, barrier 28 Å, as in Ref. 17.

$$\beta_0-\beta_1\propto\frac{2\langle z\rangle_{10}^2}{E_1^0-E_0^0}-\frac{\langle z\rangle_{21}^2}{E_2^0-E_1^0}. \tag{13}$$

As an illustration, we consider the calculated wave functions and energy levels for our samples. Since the most important contribution to the carrier redistribution is the $\beta_0-\beta_1$ term, we present $(E_1^0-E_0^0)^{-1}$ and $\langle z\rangle_{10}^2$ in Fig. 4, plotted as a function of n_0. Both functions clearly show a maximum at approximately the same value of n_S. From the self-consistently calculated wave functions, one finds that this maximum position corresponds to a front-gate bias where the electron distribution is centered with respect to the spike. In this situation, the two occupied subbands are symmetric and asymmetric states with minimum energy difference $E_1^0-E_0^0$. At the same time, the matrix element $\langle z\rangle_{10}^2$ is maximum. Generally, the inverse energy difference and the squared off-diagonal matrix element respond similarly to a changing external parameter.

We expect a less pronounced maximum for weaker potential spikes. This is confirmed in a measurement on a similar sample with a weaker potential spike, where we find a monotonic increase of $\gamma(n_S)$ (Fig. 5). We want to emphasize that even without a potential spike, the subband carrier redistribution is strongly influenced by the DOS contribution.

For arbitrary confining potentials, one has to compare relevant matrix elements and energy differences. In Table I, we present the calculated values for a heterostructure, a parabolic potential, a PQW with and without spike, and a double quantum well (DQW). In order to clarify the relative importance of the diamagnetic shift and the DOS, we split γ from Eq. (9) into the two contributions γ_{dia} and γ_{DOS}. The weaker the tunneling coupling between the left and the right side of the well, the more important the $\beta_0-\beta_1$ term becomes. In addition, this term has to be weighted by the total carrier density n_S rather than by the subband density difference. In a heterostructure, $\beta_0-\beta_1$ is negative, which weakens γ_{DOS}, such that γ_{dia} determines the carrier redistribution. The large γ_{DOS} for DQW structures is a result of the well-known effective mass change for peanut and lense shaped Fermi contours.[17]

In conclusion, we have described the $B_\parallel$ dependence of the subband density n_0 by an analytical expression, derived from second-order perturbation theory. The comparison with measurements on PQWs gives good agreement for $B_\parallel<1$ T. In contrast to earlier publications, our results are not dominated by the diamagnetic shift, but by the influence of $B_\parallel$ on the DOS of the two subbands, which leads to a redistribution of the carrier densities among the subbands. This explanation was confirmed in measurements where the shape of the confining potential could be controlled.

It should be worthwhile to check this effect by cyclotron resonance experiments, where we expect a pronounced splitting of the absorption because the effective masses in this two-subband system display a different $B_\parallel$ dispersion.

ACKNOWLEDGMENTS

We appreciate the contributions to this work by L. Roschier and M. Huberty and thank T. Ihn for fruitful discussions, and P. Studerus, A. Hermann, and B. Graf for technical assistance. We made use of a one-dimensional poisson-solver written by G. Snider. This project was financially supported by the Swiss Science Foundation and AFOSR Grant No. F 49620-94-1-0158.

[1] K. Ensslin, A. Wixforth, M. Sundaram, P.F. Hopkins, J.H. English, and A.C. Gossard, Phys. Rev. B **47**, 1366 (1993).
[2] J. C. Maan, *Two-Dimensional Systems, Heterostructures and Superlattices* (Springer, Berlin, 1984), p. 183.
[3] R. Merlin, Solid State Commun. **64**, 99 (1987).
[4] F. Stern and W.E. Howard, Phys. Rev. **163**, 816 (1967).
[5] F. Stern, Phys. Rev. Lett. **21**, 1687 (1968).
[6] S.K. Bhattacharya, Phys. Rev. B **25**, 3756 (1982).
[7] W. Zawadzki, S. Klahn, and U. Merkt, Phys. Rev. B **33**, 6916 (1986).
[8] T. Jungwirth and L. Smrcka, J. Phys.: Condens. Matter **5**, L217 (1993).
[9] J. M. Heisz and E. Zaremba, Semicond. Sci. Technol. **8**, 575 (1993).
[10] S.J. Lee, M.J. Park, G. Ihm, M.L. Falk, S.K. Noh, T.W. Kim, and B.D. Choe, Physica B **184**, 318 (1993).

[11] Jed Dempsey and B.I. Halperin, Phys. Rev. B **47**, 4662 (1993).
[12] L. Smrcka and T. Jungwirth, J. Phys.: Condens. Matter **6**, 55 (1994).
[13] D.M. Mitrinović, V. Milanović, and Z. Ikonić, Phys. Rev. B **54**, 7666 (1996).
[14] W. Beinvogl, A. Kamgar, and J. F. Koch, Phys. Rev. B **14**, 4274 (1976).
[15] J. C. Portal, R.J. Nicholas, M.A. Brummell, A.Y. Cho, K.Y. Cheng, and T.P. Pearsall, Solid State Commun. **43**, 907 (1982).
[16] S. Oelting, A.D. Wieck, E. Batke, and U. Merkt, Surf. Sci. **196**, 273 (1988).
[17] G.S. Boebinger, A. Passner, L.N. Pfeiffer, and K.W. West, Phys. Rev. B **43**, 12 673 (1991).
[18] L. Smrcka, P. Vasek, J. Kolacek, T. Jungwirth, and M. Cukr, Phys. Rev. B **51**, 18 011 (1995).
[19] G.R. Facer, B.E. Kane, R.G. Clark, L.N. Pfeiffer, and K.W. West, Phys. Rev. B **56**, 10 036 (1997).
[20] G. Salis, B. Graf, K. Ensslin, K. Campman, K. Maranowski, and A.C. Gossard, Phys. Rev. Lett. **79**, 5106 (1997).
[21] M. Shayegan, T. Sajoto, J. Jo, and M. Santos, Phys. Rev. B **40**, 3476 (1989).